International Journal of Automotive Technology, Vol. 11, No. 3, pp. 429–434 (2010)
DOI 10.1007/s12239–010–0052–y

1229–9138/2010/052–16

EFFECTS OF STACK ARRAY ORIENTATION ON FUEL CELL EFFICIENCY FOR AUXILIARY POWER UNIT APPLICATIONS

K.-S. CHOI[1)], S.-H. JANG[1)], G. S. SHIN[1)], H.-M. KIM[1)*], H. C. YOON[2)], M. E. FORREST[3)] and P. A. ERICKSON[3)]

[1)]Department of Mechanical Engineering & High Safety Vehicle Core Technology Research Center, INJE University, Gyeongnam 621-749, Korea
[2)]Institute of Energy Technology, ETH Zurich, CH-8092 Zurich, Switzerland
[3)]Department of Mechanical and Aeronautical Engineering, UC Davis One Shields Avenue, Davis, CA 95616, USA

(Received 7 August 2008; Revised 18 September 2009)

ABSTRACT–The commercial fuel cell products currently appearing on the market are self-contained fuel cell engines. These engines can be used for many applications that are presently dominated by internal combustion engines or batteries. Vehicle mounted fuel cell auxiliary power units have been attracting attention lately. Additionally, there is a market based incentive to use multiple small fuel cell arrays in place of a single large fuel cell for some applications. Typically, fuel cells are designed to operate as stand-alone units. This paper investigates the ability of small commercial stacks to operate in common array arrangements. Although an individual Nexa is able to produce 1500 W, Dual Nexas do not maintain that capability while in array configurations. With an overall load share ratio of 1.02:1 the series array reliably produced 2900 W of power, while with an overall load share ratio of 1.09:1 the parallel array reliably produced only 2800 W of power. This study shows that array orientation affects both system stack net efficiency and individual stack net efficiency. The information gained from this study may be helpful for fuel cell design and integration.

KEY WORDS : Fuel cell auxiliary power unit, Fuel cell array, Nexa power module, Array orientation, Stack net efficiency

NOMENCLATURE

ANOVA	: analysis of variation
APU	: auxiliary power unit
FC	: fuel cell
PCV	: purge cell voltage
PEM	: polymer electrolyte membrane
V_{OC}	: open circuit voltage

1. INTRODUCTION

Auxiliary power units are often installed on long-haul trucks, recreational vehicles, and military vehicles. Many of these vehicle applications require robust system with low operation noise, low exhaust emissions, high specific energy, high energy density, and flexible fuel usage. One of the more promising technologies is the PEM FC. The PEM FC is one of the six FC technologies currently being developed. The PEM FC potentially satisfies the requirements listed above except for overall system robustness and flexible fuel capability. With the steady improvement in these areas, which come with continued product maturity, PEM FCs may soon enter the APU market (Cacciola, *et al*., 2001; Zizelman *et al*., 2002; Qi and Kaufman, 2002). Despite their high cost, vehicle mounted FC APUs are attracting attention in the trucking industry and the military. Many studies have been conducted to prepare for the day when FC costs become competitive with other energy conversion technologies. The trucking industry is primarily interested in reducing idling time, fuel costs and engine wear while maintaining driver comfort when parked at rest stations. In some cases, 40% of the total time that the engine is running, is spent idling to power climate control devices and sleeper compartment accessories, as well as to avoid the start-up problems in cold weather (Brodrick *et al*., 2002). Use of FC APUs over diesel APUs offers several advantages, including general emission reductions, fuel cost savings, and economic benefits (Brodrick *et al*., 2000). Most studies on FC APU development are theoretical or are based on computer modeling (Cacciola *et al*., 2001; Zizelman *et al*., 2002; Qi and Kaufman, 2002; Brodrick *et al*., 2002, 2000; Venturi and Martin, 2001; Venturi *et al*., 2003; He *et al*., 2005). While these are important tools for refining FC APU design, the non-idealized systems have received very little attention. These studies may lack connection with the real world as products are not always used in the predicted manner or in the idealized conditions assumed in a computer model. Real

**Corresponding author.* e-mail: mechkhm@inje.ac.kr

world usage often involves operational validity, external perturbation, and application integration. Furthermore, hardware testing is an invaluable means of identifying false assumptions. One of the assumptions that are made in many FC engine computer models is that the right size stack is always available. Not every FC APU company produces their own stacks in-house, nor are there production line FC engines that can meet the power requirements of every application. One way to avoid this problem is to utilize an array of FC engines rather than a single FC engine that must be just the right size.

Whether or not multiple small relatively affordable FC engines combined into arrays can perform as well as a single idealized FC engine is currently unknown (Read *et al.*, 2001). The Nexa power module (Ballard Power Systems) was selected for this study because it is widely used. However, the results of this study are likely not unique to the Nexa FC. When considering the consequences of operating arrays of fuel cell engines, it was important to consider issues involving the duplicated balance of the plant. In the present study, the sensitivity of the FC system to dual-stack parallel and the series array operation was investigated experimentally. The net efficiencies were calculated and compared using ANOVA. Finally, the importance of stack matching and the impact of stack matching on load sharing were discussed.

2. EXPERIMENTAL FACILITY AND APPROACH

The Nexa FC engine is rated by Ballard Power Systems Inc. to produce 1200 W, with a rated current of 46 A at 26 V. The Nexa FC is composed of 47 cells in series. The specified operational voltage range is 22~50 V, the operating temperature range is 3°C to 30°C, and the operational humidity range is 0% to 95%. Because of the low volume of hydrogen purged during normal use, it is rated for both indoor and outdoor use (Ballard Power Systems, 2004).

Figure 1 shows a schematic of the primary wiring plug connectors on the FCs. The Nexa is a self-contained FC engine, requiring only a hydrogen supply and a small external power source to facilitate start-up and shutdown. A brass board provided a means with which to test the Nexa FCs in single, parallel, or series stack arrangement. Changing from one arrangement to another involved plugging the Nexa into the brass board in the proper arrangement and connecting the appropriate load to the brass board. Two Hall Effects sensors for measuring the net stack currents and two voltage dividers for measuring the system and the stack voltages were incorporated into a data acquisition board. Signals from these components were acquired using hardware and software from National Instruments. A PCI-MIO-16E-4 card was used in an x86 computer running LabVIEW 6.1. Analog inputs were sampled at a burst rate of 35 kHz, and the samples were then averaged at a sample size of 925-samples. The Nexa on-board control and diagnostic system collects a wide variety of data for monitoring the FC stack, including the gross current, voltage, power, stack and ambient temperatures, purge voltage, stoichiometry, fan duty-cycles, and error information.

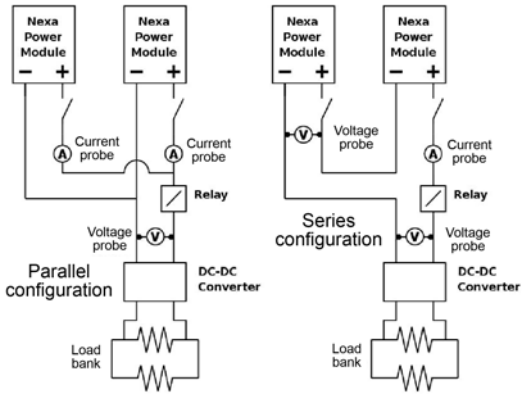

Figure 1. Schematic of the primary wiring plug connecto on the FCs.

Because of the difference in the system voltage between the parallel and series array, a constant power loading scheme was used. Preliminary testing of the Nexa stacks showed that each stack was able to put out 0 A-to-60 A over a voltage range of 43 V-to-25 V. This suggests that two Nexas should be able to provide 3 kW of power. However, because of the uncertainty in the performance of two Nexas in any array configuration, 3 kW of power was simply a best guess. A load schedule containing randomized load set-points, ranging from 0.1 kW to 3 kW in increments of 0.1 kW, was created. We expected that some of the highest set-points might need to be removed to allow both arrays to successfully complete at least two runs. When a particular set-point caused an array to fail more than one of its runs, the offending set-point was removed and replaced with a 0.0 kW set-point. The preliminary load schedule for testing the Dual Nexa is given in Table 1.

To ensure repeatability, both phases of Nexa testing were preceded by a warm-up period to ensure that the stacks were up to steady state temperature. A warm-up period of 1 kW constant power for 360 sec was adequate for bringing the stacks up to temperature and allowing the stack temperature to cycle between the control limits for at least one full cycle. At the conclusion of each test, the Nexas were manually shut down to ensure that all of the water

Table 1. Load schedule for the dual Nexa testing.

Step	1	2	3	4	5	6	7	8	9	10	11	12	13	14	15
Set point (kW)	1.6	0.5	2.5	0.9	3.0	1.2	2.9	1.9	0.2	1.0	2.2	0.7	0.6	1.5	2.8
Step	16	17	18	19	20	21	22	23	24	25	26	27	28	29	30
Set point (kW)	0.8	2.1	1.7	1.3	0.3	2.7	0.1	1.4	2.4	1.8	2.3	2.6	0.4	2.0	1.0

produced during the run was purged from the stack before initiating the next run.

Data analysis was performed in three phases. In the first phase, net and gross data files were aligned by synchronizing all of the set-point transitions. In the next phase, the demand for net efficiency, maximum power and auxiliary power was calculated. Breaking down the auxiliary power demand into individual component demands required the use of Regression Analysis. In the final phase, ANOVA was used to test the effect of the control variables on net efficiency (J. Neter, *et al*., 1996). ANOVA calculates an F distribution as defined below:

$$F = \frac{Mean\_Square_{factors}}{Mean\_Square_{errors}} \quad (1)$$

The F value reflects the significance of the effect of variable on net efficiency. To perform ANOVA analysis, a statistical package program (SAS) was used. All calculations were performed using a 95% level of confidence.

Each fuel cell stack has its own unique polarization curve, which indicates the amount of power the stack will produce for a given voltage or current. By joining stacks into arrays, particular parameters of the polarization curves are bound together; the series arrays bind the net currents, and the parallel arrays bind the net voltages. The Nexas used in this study were well matched but not perfectly matched. As a result, differing polarization curves introduced unequal load sharing. The load sharing for each array was quantified by calculating the load share ratio as follows:

$$\frac{\Sigma(A/B)}{n} : \frac{\Sigma(B/B)}{n} \quad (2)$$

where A and B designate the power output of the stronger and weaker stacks at a particular time period, respectively; n represents the total number of samples taken during the time period (EG&G Technical Services Inc., 2002).

3. RESULTS AND DISCUSSION

3.1. Maximum Power of Dual Stack Arrays

Although an individual Nexa power module is able to produce 1500 W, they do not maintain that capability while in array configurations. Both series and parallel arrays failed under a 3000 W load because of a sustained low purge cell voltage or an over-current condition. When connected to 2900 W loads, all of the series runs were completed successfully, and all of the parallel runs failed because of an over-current.

Table 2 provides a typical example of a series stack failure caused by a sustained low purge cell voltage during a 3000 W test. The currents and voltages were within reason, but the purge cell voltage combined for the series stack remained below 1.10 V for longer than 20 sec. In applications not using the NexaMon program to monitor the purge cell voltage, the operator would get no warning that a stack failure due to low purge cell voltage is about to occur. Even with such monitoring, the only way to avert such a failure would be to reduce the load on the FC array by an amount sufficient to raise the purge cell voltage above 1.10 V.

Table 2. Typical examples of a series stack failure during a 3000 W set-point.

	Power (W)	Current (A)	Voltage (V)	PCV (V)	Failure
Nexa-570	1509	55.9	27.0	1.12	No
Nexa-592	1487	55.9	26.6	1.09	Yes
Series array	2996	55.9	53.6	N/A	Yes

Table 3. Typical examples of an imminent (0.06 s) failure during a parallel FC array test.

	Power (W)	Current (A)	Voltage (V)	PCV (V)	Failure
Nexa-570	1514	64.81	23.36	1.11	No
Nexa-592	1390	59.52	23.36	1.00	No
Parallel array	2904	124.3	23.36	N/A	No

Table 3 illustrates a typical parallel test that showed that the Nexas could provide 2900 W, but only for a fraction of a second. Providing the power during the overshoot period required the stronger stack to produce current in excess of the 60 A maximum limit. Had the maximum current limit been exceeded for longer than 1 sec, the Nexa would have shutdown due to an over-current failure.

Unlike the failure of the series array above, a failure of a parallel array could be predicted using commonly available current and voltage sensors. As was the case with the series array, the only way to avert operational stack failure was to reduce the load on the FC array.

3.2. Effects of Dual Stack Array Orientation on Net Efficiency

Using the maximum sustainable power level, the randomized load schedule given in Table 1 was used to test both the series and parallel arrays. Although neither array experienced an operational stack failure during the preliminary testing, one failure did occur during the randomized load-level testing. Representative power curves for the parallel and series arrangements are given in Figures 2 and 3, respectively.

Overall, two dynamics occur during the operation of both arrays. First, there is a fairly constant load sharing ratio, where the Nexa with the higher polarization curve produces more of the power. Second, the fluctuating partial pressure of hydrogen within the two Nexas causes an instantaneous load sharing ratio to vary with time. A summary of all the parallel and series run results are given in Tables 4 and 5, respectively.

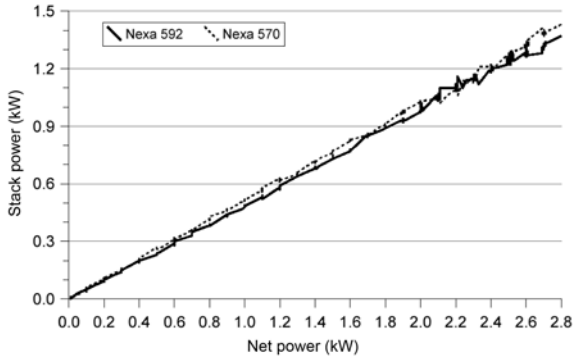

Figure 2. Representative power curves and load sharing for the parallel arrangement.

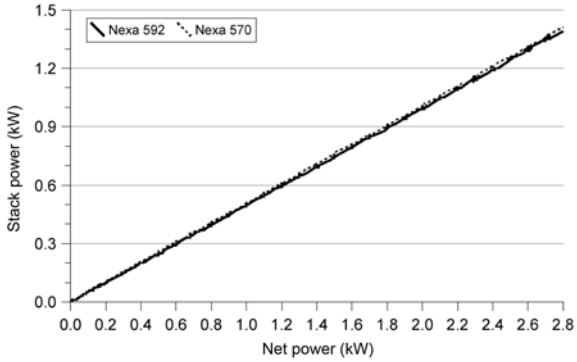

Figure 3. Representative power curves and load sharing for the series arrangement.

Despite appearing essentially identical, as shown in Tables 4 and 5, there is a statistical difference in net efficiency between the two array arrangements, as shown in Tables 6, 7, and 8.

The F-Test results in Tables 6, 7, and 8 show that the difference in net efficiency between the parallel and series

Table 4. Summary and net efficiency data of all of the parallel run results.

Run	Successfully completed runs						Failed run		
	P1			P3			P2		
Nexa	N-570	N-592	Parallel	N-570	N-592	Parallel	N-570	N-592	Parallel
Average gross current (A)	23.9	23.11	47.01	23.78	23.23	47.01	23.18	22.28	45.47
Average net power (W)	661.35	640.82	1303.12	654.14	648.66	1302.81	640.2	617.86	1259.18
Run time (s)	870			870			749		
ΔH (W, HHV)	1,664	1,609	3,273	1,656	1,617	3,273	1,614	1,551	3,166
Net efficiency (%, HHV)	39.74	39.83	39.81	39.5	40.12	39.8	39.67	39.84	39.77

Table 5. Summary and net efficiency data of all of the series run results.

Run	Successfully completed runs								
	S1			S2			S3		
Nexa	N-570	N-592	Series	N-570	N-592	Series	N-570	N-592	Series
Average gross current (A)	23.2	23.05	23.2	23.1	22.97	23.1	23.33	23.21	23.33
Average net power (W)	656.5	647.12	1303.61	656.01	647.61	1303.62	655.55	648.05	1303.6
Run time (s)	870			870			870		
ΔH (W, HHV)	1,615	1,605	3,230	1,608	1,599	3,216	1,624	1,616	3,248
Net efficiency (%, HHV)	40.65	40.32	40.36	40.8	40.5	40.54	40.37	40.1	40.14

Table 6. Table-System Net Efficiency: dependent variable: system, number of variables 6.

Source	DF	Sum of squares	Mean square	F value	Probability>F
Model	1	0.4411067	0.4411067	22.62	0.0089
error	4	0.0779906	0.0194977		
corrected total	5	0.5190973			
	R-Square	Coeff var	Root MSE	System mean	
	0.849757	0.348453	0.139634	40.07257	
Source	DF	Type I SS	Mean square	F value	Probability>F
Arrangement	1	0.4411067	0.4411067	22.62	0.0089

Table 7. Table-NEXA 570 Net Efficiency: dependent variable: NEXA 570, number of variables 6.

Source	DF	Sum of squares	Mean square	F value	Probability>F
Model error	1	1.9021912	1.9021912	27.98	0.0061
corrected total	4	0.2719629	0.0679907		
	5	2.1741541			
	R-square	Coeff var	Root MSE	System mean	
	0.874911	0.648541	0.26075	40.20568	
Source	DF	Type I SS	Mean Square	F Value	Probability>F
Arrangement	1	1.9021912	1.9021912	27.98	0.0061

Table 8. ANOVA Table-NEXA 592 Net Efficiency: dependent variable: NEXA 592, number of variables 6.

Source	DF	Sum of squares	Mean square	F value	Probability>F
Model error	1	0.0781146	0.0781146	4.16	0.1109
corrected total	4	0.0781146	0.0187624		
	5	0.1531644			
	R-square	Coeff var	Root MSE	System mean	
	0.510005	0.342138	0.136976	40.03532	
Source	DF	Type I SS	Mean square	F value	Probability>F
Arrangement	1	0.0781146	0.0781146	4.16	0.1109

arrays was more significant for the Nexa-570 than for the Nexa-592. This is a consequence of the overall load sharing between the two Nexas.

The average load sharing ratios for the series and parallel arrays were 1.02:1 and 1.09:1, based on Tables 2 and 3, respectively. The discrepancy explains why the series array was able to sustain a 2900 W load, while the parallel array was only able to sustain a 2800 W load. The difference in maximum sustainable load is due to the different parameter bounds in each array orientation. With current as the limiting factor at high power production levels, binding the currents together in the series array ensures that each stack reaches the maximum current limit at the same time. This forced the weaker stack to produce its fair share of the work.

In contrast, binding voltages together will force the stack with the stronger polarization curve to produce more power because it will produce more current at a given voltage. Thus, at maximum powers, the stronger stack in a parallel array will approach the maximum current limit before the weaker one.

While the polarization curves had the strongest influence on the overall load sharing, there were some other factors. This is evidenced by the variability in the instantaneous load sharing, as indicated by the rough appearance of the curves in Figures 2 and 3. This roughness is a result of the change in partial pressure of hydrogen at the anodes of the Nexas, which in turn affects the stack voltage. The frequency of the voltage oscillation is dependent on the level of power production and the frequency of the anode purges. At higher levels of power production the period of purge oscillation is fairly high, on the order of 30 sec; at lower levels the period of the purge oscillation is about 2 min. The stack power for a given load level, at the right side of the curves, is scattered because almost the entire voltage oscillation occurs during the sampling period. This makes those portions of the curves appear rougher. At lower power levels, only a portion of the voltage oscillation occurred during the sampling period. This makes that section of the curve appear smoother. The oscillations occurred asynchronously for series arrays and synchronously for parallel arrays, which is why the effect was more pronounced in Figure 2. The effective array voltage oscillation for the parallel array is almost twice as much as it is for the series array.

One of the potential concerns for running mismatched fuel cells in parallel is the likelihood of reverse currents from the stronger stack into the weaker one. As soon as two stacks with differing open circuit voltages are connected in parallel a current loop is created, even before a load is applied. The amount of current flow can be found if both the polarization curve of the stronger stack and the resulting system voltage are known. In this study, one Nexa's average V_{OC} was 1.4 V higher than the other. When connected in parallel, the voltage of the stronger stack dropped by 0.7 V, the voltage of the weaker one increased by 0.7 V, and a negative current of about 2.8 A began flowing into the weaker stack. With a V_{OC} of 42.0 V, 117.6 W of power was dissipated by the weaker stack. We do not know how this condition would affect the lifespan of the weaker stack

if it were to occur over a long period of time.

4. CONCLUSIONS

The sensitivity of an FC system to dual-stack parallel and series array operation was investigated experimentally. Although an individual Nexa FC is able to produce 1500 W, two Nexas in an array configuration could not produce 3000 W because of unequal load sharing. With an overall load share ratio of 1.02:1, the series array reliably produced 2900 W of power, while with an overall load share ratio of 1.09:1, the parallel array reliably produced only 2800 W of power. We have shown that array orientation significantly affects both the system net efficiency and the individual stack net efficiency. The system net efficiency is lower for the parallel arrangement than for the series arrangement because connecting the stacks in parallel equalizes the stack voltages. The weaker stack depresses the polarization curve of the stronger stack, while the stronger stack boosts the polarization curve of the weaker stack. Finally, even though the Nexas used in this study were well matched, arranging them in parallel produced a reverse current between the two stacks. The power flowing between the two stacks was approximately 118W in the open circuit. The effects of this reverse current on the lifespan of the weaker stack should be investigated in future studies.

ACKNOWLEDGEMENT–This work was supported by the National Research Foundation of Korea (NRF) grant funded by the Korea government (MEST) (No. 2009-0080496).

REFERENCES

Ballard Power Systems (2004). *Nexa Power Module Specification Sheet* [online]. Ballard Power System Inc. Available from: http://www.ballard.com/resources/powergen/NexaSpecSheet.pdf [accessed 11 Dec 2006]

Brodrick, C. J. (2002). Evaluation of fuel cell auxiliary power units for heavy-duty diesel trucks. *Transportation Research-Part D* **7**, **4**, 303–315.

Brodrick, C. J. (2000). Demonstration of a proton exchange membrane fuel cell as an auxiliary power source for heavy trucks. *SAE Paper No*. 2000-01-3488.

Cacciola, G., Antonucci, V. and Freni, S. (2001). Technology up date and new strategies on fuel cells. *J. Power Sources* **100**, **1–2**, 67–79.

EG&G Technical Services, Inc. (2002). *Fuel Cells: A Handbook*. 6th Edn. US Department of Energy. Illinois.

He, B., Ouyang, M. and Lu, L. (2005). Modeling and PI control of diesel APU for series hybrid electric vehicles. *Int. J. Automotive Technology* **7**, **1**, 91–99.

Neter, J., Kutner, M. H., Nachtsheim, C. J. and Wasserman, W. (1996). *Applied Linear Statistical Models*. 4th Edn. McGraw-Hill. Boston.

Qi, Z. and Kaufman, A. (2002). PEM fuel cell stacks operated under dry-reactant conditions. *J. Power Sources* **109**, **2**, 469–476.

Read, C. J., Jan, H. J., Thijssen, S. and Carlson, E. J. (2001). Fuel cell auxiliary power systems: Design and cost implications. *SAE Paper No*. 2001-01-0536.

Venturi, M. and Martin, A. (2001). Liquid-fueled APU fuel cell system for truck application. *SAE Paper No*. 2001-01-2716.

Venturi, M., Kallio, E., Smith, S. and Baker, J. (2003). Recent results on liquid-fuelled APU for truck application. *SAE Paper No*. 2003-01-0266.

Zizelman, J., Shaffer, S. and Mukerjee, S. (2002). Solid oxide fuel cell auxiliary power unit - A development update. *SAE Paper No*. 2002-01-0411.